

Life in the PFAS lane: The impact of perfluoroalkyl substances on photosynthesis, cellular exudates, nutrient cycling, and composition of a marine microbial community



Sarah N. Davis ^{a,*}, Shaley M. Klumker ^a, Alexis A. Mitchell ^a, Marshall A. Coppage ^b, Jessica M. Labonté ^a, Antonietta Quigg ^{a,c,d}

^a Department of Marine Biology, Texas A&M University at Galveston, 200 Seawolf Parkway, Galveston, TX 77553, USA

^b Department of Biological Sciences, University of South Carolina, 715 Sumter Street, Columbia, SC 29208, USA

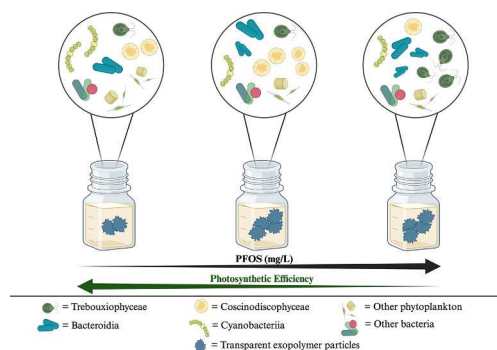
^c Department of Oceanography, Texas A&M University, 3146 TAMU, College Station, TX 77843, USA

^d Department of Ecology and Conservation Biology, Texas A&M University, 534 John Kimbrough Boulevard, College Station, TX 77843, USA

HIGHLIGHTS

- Impact of PFOS and 6:2 FTS exposure on a marine microbial community was evaluated.
- Phytoplankton photosynthesis was disrupted when exposed to PFOS, but not 6:2 FTS.
- PFOS increased TEP release indicating heightened microbial stress.
- PFOS exposure lowered microbial (phytoplankton, bacteria) diversity and evenness.
- PFOS caused more variation in eukaryotic versus prokaryotic community composition.

GRAPHICAL ABSTRACT



ARTICLE INFO

Editor: Jay Gan

Keywords:

Phytoplankton
Marine microbial communities
PFOS
6:2 FTS
Transparent exopolymer particles (TEP)
Photophysiology

ABSTRACT

Perfluoroalkyl substances (PFAS) are of great ecological concern, however, exploration of their impact on bacteria-phytoplankton consortia is limited. This study employed a bioassay approach to investigate the effect of unary exposures of increasing concentrations of PFAS (perfluorooctane sulfonate (PFOS) and 6:2 fluorotelomer sulfonate (6:2 FTS)) on microbial communities from the northwestern Gulf of Mexico. Each community was examined for changes in growth and photophysiology, exudate production and shifts in community structure (16S and 18S rRNA genes). 6:2 FTS did not alter the growth or health of phytoplankton communities, as there were no changes relative to the controls (no PFOS added). On the other hand, PFOS elicited significant phototoxicity ($p < 0.05$), altering PSII antennae size, lowering PSII connectivity, and decreasing photosynthetic efficiency over the incubation (four days). PFOS induced a cellular protective response, indicated by significant increases ($p < 0.001$) in the release of transparent exopolymer particles (TEP) compared to the control. Eukaryotic communities (18S rRNA gene) changed substantially ($p < 0.05$) and to a greater extent than prokaryotic communities (16S rRNA gene) in PFOS treatments. Community shifts were concentration-dependent for

* Corresponding author.

E-mail address: snadavis1@tamu.edu (S.N. Davis).

eukaryotes, with the low treatment (5 mg/L PFOS) dominated by Coscinodiscophyceae (40 %), and the high treatment (30 mg/L PFOS) marked by a Trebouxiophyceae (50 %) dominance. Prokaryotic community shifts were not concentration dependent, as both treatment levels became depleted in Cyanobacteriia and were dominated by members of the Bacteroidia, Gammaproteobacteria, and Alphaproteobacteria classes. Further, PFOS significantly decreased ($p < 0.05$) the Shannon diversity and Pielou's evenness across treatments for eukaryotes, and in the low treatment (5 mg/L PFOS) for prokaryotes. These findings show that photophysiology was not impacted by 6:2 FTS but PFOS elicited toxicity that impacted photosynthesis, exudate release, and community composition. This research is crucial in understanding how PFOS impacts microbial communities.

1. Introduction

Perfluoroalkyl substances (PFAS) are a large class of synthetic chemicals, composing >14,000 identified compounds (U.S. EPA, 2022). They are widely used in common products such as liquid repellents including surfactants, coatings, and aqueous film forming foams (Ahrens and Bundschuh, 2014). Some PFAS are extremely stable, resisting chemical and biological degradation due to the strong carbon-fluorine bonds comprising their structure (Prevedouros et al., 2006). This structural stability has made many PFAS favorable for commercial and industrial uses, but this design also results in them being persistent, non-degradable chemicals in the environment (Gaines et al., 2023). This engenders a great deal of concern, as the use and manufacturing of PFAS products has resulted in their release into the environment during product life cycle (Prevedouros et al., 2006; Ahrens and Bundschuh, 2014). In turn, this has led to PFAS contamination in global ecosystems (Rankin et al., 2016; Muir and Miaz, 2021; Podder et al., 2021) with aquatic environments more vulnerable to PFAS contamination, as waterways are suggested as their final sink (Prevedouros et al., 2006). PFAS now contaminate diverse aquatic ecosystems including lakes (Lam et al., 2014; Zhang et al., 2022), rivers (Lam et al., 2014; Ramírez-Canon et al., 2022; Viticoski et al., 2022), estuaries (Naile et al., 2010; Nolen et al., 2022; Novak et al., 2023), and coastal seas and oceans (Muir and Miaz, 2021). Depending on the location, PFAS are often detected at up to ng/L levels (Muir and Miaz, 2021; Podder et al., 2021), but industrial activities, or the use of aqueous film forming foams, can lead to higher environmental concentrations from ug/L to mg/L PFAS (Aly et al., 2020; Masoner et al., 2020; O'Carroll et al., 2020; Nolen et al., 2022).

Of particular concern is the dominant PFAS compound perfluorooctane sulfonate (PFOS), which is ubiquitously detected in the environment (Muir and Miaz, 2021; Podder et al., 2021). PFOS is persistent (Ahrens and Bundschuh, 2014; Beach et al., 2006) and shown to bioaccumulate in biota (Conder et al., 2008; Casal et al., 2017; Nolen et al., 2022, 2024). Following contamination of ecosystems, PFOS may disrupt biological processes and is observed to elicit a wide range of toxic effects on aquatic species, including inhibiting growth (Boudreau et al., 2003; Simpson et al., 2021; Krupa et al., 2022), disrupting reproduction (Simpson et al., 2021; Krupa et al., 2022) and increasing oxidative stress in organisms (Lim, 2022; Ma et al., 2023). In recent decades, knowledge of PFOS toxicity, persistence, and widespread contamination has led to a necessary shift in manufacturing of chemical substitutes (Field and Seow, 2017). 6:2 fluorotelomer sulfonate (6:2 FTS) is a common substitute to PFOS and is similarly detected in global aquatic ecosystems (Coggan et al., 2019; Cheng et al., 2023; Novak et al., 2023), in some instances at higher concentrations than PFOS (Nguyen et al., 2019; Aly et al., 2020). To date, 6:2 FTS is thought to be less toxic than legacy PFAS; it has been documented to pose minimal risk to aquatic organisms and not bioaccumulate (Hoke et al., 2015). Nevertheless, toxicological assessments of legacy PFAS, as well as assessments of emerging PFAS, are pertinent to provide holistic toxicity data, particularly regarding aquatic flora and fauna.

Phytoplankton and bacteria are vital in aquatic food webs as primary producers and degraders (Seymour et al., 2017). Disruptions to their productivity and diversity can impact biogeochemical cycles (Cotner and Biddanda, 2002; Litchman et al., 2015) and the abundance or

diversity of higher aquatic organisms (Chassot et al., 2007). Further, phytoplankton and bacteria are intrinsically linked, working in tandem through complex microbial interactions; relationships between the two groups maintaining the ecosystem functions they both provide (Seymour et al., 2017). Microbes, herein used to refer to phytoplankton and bacteria, have been shown to be vulnerable to pollution (Doyle et al., 2018, 2020; Kamalanathan et al., 2019, 2021). Further, microbes inhabiting estuarine and coastal environments undergo increased exposure to pollutants, as these habitats are closely associated with anthropogenic activities. For this reason and others, it is imperative to elucidate the effects of the contaminants PFOS and 6:2 FTS on coastal microbial communities.

Recent laboratory-based microbial studies revealed that PFOS increases cell membrane permeability (Rodea-Palomares et al., 2012; Xu et al., 2017; Fitzgerald et al., 2018), damages photosynthetic machinery (Xue et al., 2022), alters pigment concentrations and ratios (Xu et al., 2017; Muhammad et al., 2023; Zhang et al., 2023a), hinders growth (Boudreau et al., 2003; Liu et al., 2016; Xue et al., 2022; Muhammad et al., 2023), and causes oxidative stress (Liu et al., 2016; Xu et al., 2017; Xue et al., 2022). Few studies have concomitantly compared unary exposures of 6:2 FTS and PFOS toxicity on microbial communities; however, a recent report by Zhang et al. (2023a) found that PFOS elicited a greater toxic effect on growth, chlorophyll (chl) *a* content, and photosynthesis compared to 6:2 FTS. Literature investigating the impacts of PFOS or 6:2 FTS have mainly concentrated on monoculture studies utilizing phytoplankton species (Boudreau et al., 2003; Liu et al., 2008, 2009; Rodea-Palomares et al., 2012; Xu et al., 2017; Xue et al., 2022; Muhammad et al., 2023; Zhang et al., 2023a), which leads to limitations in extrapolating these findings to complex and diverse natural environments. Though recent studies have begun to bridge monoculture findings with complex ecosystems by considering PFAS effects on microbial consortiums, these have primarily focused on bacterial assemblages (Cai et al., 2020; Cerro-Gálvez et al., 2020; Guo et al., 2023; Qiao et al., 2018) and simulated algae-bacteria communities (Wu et al., 2022b), but have not assessed a natural phytoplankton-bacterial community.

The aim of this study was to investigate the impact of PFOS and 6:2 FTS on natural microbial communities collected from the coastal zone of the Gulf of Mexico. Using a bioassay approach and unary exposures, we compared how PFOS and 6:2 FTS impacted the growth and photosynthesis of phytoplankton communities. Subsequently, we investigated PFOS disruption of the microbial production of stress molecules, nutrient cycling, and the diversity of prokaryotic and eukaryotic communities. Our primary interest was to examine the health of phytoplankton exposed to PFOS and 6:2 FTS. 6:2 FTS was not found to inhibit growth and photosynthesis; hence, our secondary interest was examining microbial stress response(s) and community shifts in response to PFOS exposure.

2. Methods

2.1. Treatment preparation

1 g of heptadecafluorooctanesulfonic acid (PFOS, purity: $\geq 97\%$; Santa Cruz Biotechnology, Inc.) and 1 g of 1H, 1H, 2H,

perfluorooctanesulfonic acid (6:2 FTS, purity: 97 %; Synquest Laboratories) were dissolved in 3 mL and 1 mL of reagent grade dimethyl sulfoxide (DMSO), respectively. They were then transferred to methanol-washed polypropylene bottles; using ultrapure water the final nominal stock concentration was prepared as 1 g/L (PFOS) and 8 g/L (6:2 FTS) and stored at 4 °C. The final concentration of DMSO (0.006 % v/v) did not affect the toxicity tests (Bérard, 1996).

2.2. Bioassay collections

Two bioassays were performed using natural communities from surface waters (top 1 m) of the Gulf of Mexico collected along the coast of Galveston Island, Texas (29°15' N, 94°49' W) in July (2021) and June (2023). Seawater was collected in a pre-cleaned 20 L carboy washed in triplicate with site water. In situ temperature, salinity, and pH were measured using a calibrated water quality multiprobe (Hydrolab MS 5, Hach, Loveland, CO). Within an hour, the seawater was transported to the laboratory at Texas A&M University at Galveston and sieved (118 µm) to exclude zooplankton and limit grazing within the bioassays. The resulting seawater was gently mixed, and aliquots were distributed into 1 L sterilized and acid-washed polypropylene bottles.

Bioassays using the natural communities collected in July (2021) were exposed to PFOS [Control, 2.5, 5, 10, 20, 30 mg/L] and those conducted in June (2023) were exposed to 6:2 FTS [Control, 5, 10, 20, 40, 80 mg/L]. All concentrations are reported as nominal, and treatments were performed in triplicate. The PFOS concentrations selected for the assay were based on preliminary findings (unpublished) observing significant impacts to photosynthesis within this exposure range. Subsequently, nominal concentrations of 6:2 FTS fell within the tested PFOS concentrations and extended to higher levels (e.g., 40 and 80 mg/L) based on literature observing 6:2 FTS impacting phytoplankton at higher concentrations than PFOS (Zhang et al., 2023a).

Bioassays were deployed in a floating corral attached to the Texas A&M University at Galveston boat basin. The floating corral allows natural communities to continue to experience wave and tidal motions, natural temperature cycles, and ambient diel light (Williams et al., 2017); with a shade cloth used to reduce surface sunlight by up to 50 %. Exposure response was monitored over 4 days (96 h) by removing aliquots from each triplicate every morning between 10:00–12:00 h. Biomass and photophysiological measurements were performed daily for the PFOS and 6:2 FTS bioassays. Given that we observed changes in these parameters in the PFOS but not 6:2 FTS treatments, further measurements were not performed for the 6:2 FTS bioassay. Transparent exopolymer particles (TEP) and nutrients were measured for the control treatment on Day 0 (prior to exposure), and for all treatments on Days 2 and 4 of the PFOS bioassay. rRNA gene sequencing was performed on a subset of samples, the control collected on Day 0, and the control, 5 mg/L and 30 mg/L PFOS, collected on Day 4. Within the context of this study, two treatments will be referred to as low (5 mg/L) and high (30 mg/L), respectively, when describing the findings of the rRNA gene sequencing data for the PFOS bioassays.

2.3. Biomass and photophysiological measurements

Samples (4 mL) were collected and dark acclimated for 15 min prior to analysis on a 10 AU Turner Designs fluorometer (Turner Designs, San Jose, CA) calibrated using EPA method 445.0 (Arar and Collins, 1997). Calibration was performed with extracted *Anacytis nodulans* chlorophyll-a powder (Sigma-Aldrich) diluted in 90 % acetone at concentrations between 0 and 40 µg/L. Total in situ chlorophyll-a concentrations were used as a proxy of phytoplankton biomass (Huot et al., 2007).

Subsequently, the same aliquots were dark acclimated once more for 15 min and the photosynthetic efficiency and total health of photosystem II (PSII) were measured using a Satlantic Fluorescence Induction and Relaxation (FIRE) fluorometer (Satlantic, Halifax, Canada). We used only the information from the single turnover component of the

transient, calculated after 60 iterations (Kolber et al., 1998). Dark acclimation allows photosynthetic reaction centers to open, ensuring that baseline fluorescence (F_0) of PSII can be acquired. The FIRE system exposes phytoplankton cells to saturating pulses of blue light to yield a maximum fluorescence value (F_m). The variable fluorescence (F_v) is then calculated ($F_m - F_0$) and changes of F_v relative to F_m (F_v/F_m) represent the PSII quantum yield, a proxy of photosynthetic efficiency. The system also measures PSII functional absorption cross section (σ_{PSII} ; Å² quanta⁻¹), the minimum turnover time of electron transfer between reaction centers (τ_{PSII} ; µsec) and the connectivity factor defining the excitation energy transfer between individual photosynthetic units (ρ). These four parameters are frequently used as physiological markers when working with natural samples (Sylvan et al., 2007; Moore et al., 2008; Quigg et al., 2011).

2.4. Transparent exopolymer particles

Transparent exopolymer particles (TEP) were measured according to Passow and Alldredge (1995) with the calibration developed by Bittar et al. (2018) using Xanthan Gum as a standard. Briefly, samples were gently filtered through Isopore polycarbonate (0.4 µm) hydrophilic membrane filters and the volume for each was adjusted between treatments depending on the concentration of suspended particulate matter. Following filtration, the filter was washed with deionized water to discard excess salts, stained with calibrated Alcian blue solution (0.2 g/L in 0.06 % v/v acetic acid), and quickly rinsed with deionized water to remove excess dye. Filters were frozen (-20 °C) until extraction by homogenization in 6 mL of 80 % H₂SO₄ and measured at 787 nm on a Shimadzu UV-VIS recording spectrophotometer. TEP was quantified based on the correlation between the absorbance of the samples compared to the Xanthan Gum standard and was expressed as µg-XG equivalent/L.

2.5. Dissolved nutrients

Water samples (100 mL) were filtered using Whatman glass fiber filters (0.7 µm) to remove particulate matter and the filtrate was stored at -20 °C until analysis by the Texas A&M University Geochemical and Environmental Research Group. Concentrations of dissolved nitrate (NO₃⁻), nitrite (NO₂⁻), urea, ammonium (NH₄⁺), phosphate (HPO₄²⁻), and silicate (SiO₂) were determined on a Lachat QuikChem AE autoanalyzer. Dissolved nutrients are expressed as µmol/L and dissolved inorganic nitrogen (DIN) to phosphorus (DIN:P) ratios were calculated by first summing NO₃⁻, NO₂⁻, and NH₄⁺ to calculate the concentration of DIN.

2.6. 16S and 18S rRNA gene community analysis

Both 16S and 18S rRNA genes were analyzed to comprehensively assess the microbial community. Water samples were filtered on 0.2 µm hydrophilic polycarbonate membrane filters and stored immediately at -80 °C. DNA extractions and PCR amplification and sequencing were performed by Research and Testing Laboratory Genomics (RTL Genomics Lubbock, TX, USA). Total DNA was extracted using the Zymo-BIOMICS™ 96 MagBead DNA Kit (Zymo) for the prokaryotes (prior to 16S rRNA gene amplification) and using the DNeasy PowerWater Kit (Qiagen) for the eukaryotes (prior to 18S rRNA gene amplification), both following the manufacturer's instructions. PCR amplifications targeted the V4 regions for prokaryotes, with primer pair, 515F (5'-GTGCCAGCMGCCGCGTAA-3') and 806R (5'-GGACTTACHVGGGTCTTAAT-3') (Caporaso et al., 2011) and the V8-V9 for eukaryotes, with the primer pair, V8f (5'-ATAACAGGTCTGTATGCCCT-3') and 1510r (5'-CCTTCYGCAGGTTCACCTAC-3') (Bradley et al., 2016).

All samples were sequenced on Illumina MiSeq platform (RTL Genomics, Lubbock, TX, USA). 16S and 18S rRNA sequence reads were processed individually using mothur v1.48.0 following the MiSeq SOP (https://mothur.org/wiki/miseq_sop/ (Schloss et al., 2009; Kozich et al.,

Table 1

PSII re-oxidation time (τ_{PSII} , μsec), PSII antenna size (σ_{PSII} , \AA^2 (quanta) $^{-1}$), PSII connectivity factor (ρ , dimensionless), PSII quantum yield (Fv/Fm, unitless) and chlorophyll *a* concentrations ($\mu\text{g/L}$) of natural phytoplankton communities exposed to PFOS treatments (Control, 2.5, 5, 10, 20, 30 $\mu\text{g/L}$). Results expressed as mean (standard deviation) and significance is noted as follows, ‘***’ 0.001, ‘**’ 0.01, ‘*’ 0.05.

	τ_{PSII}	ρ	σ_{PSII}	Fv/Fm	chl <i>a</i>
Day 0					
Control	352 (44.0)	0.39 (0.01)	197.0 (1.7)	0.56 (0.003)	1.55 (0.01)
2.5	338 (33.3)	0.37 (0.03)	193.3 (2.3)	0.57 (0.007)	1.53 (0.08)
5	320 (12.5)	0.34 (0.01)	197.0 (2.7)	0.56 (0.003)	1.53 (0.08)
10	276 (9.8)	0.35 (0.01)	196.3 (3.2)	0.56 (0.003)	1.49 (0.02)
20	313 (29.6)	0.35 (0.02)	197.3 (3.1)	0.56 (0.006)	1.47 (0.01)
30	286 (29.8)	0.34 (0.04)	195.3 (5.0)	0.56 (0.006)	1.43 (0.07)
Day 1					
Control	306 (11.7)	0.22 (0.01)	215.0 (9.0)	0.54 (0.025)	2.65 (0.03)
2.5	287 (10.1)	0.20 (0.02)	215.3 (10.4)	0.56 (0.018)	2.69 (0.23)
5	345 (47.9)	0.22 (0.03)	214.0 (11.4)	0.54 (0.010)	2.82 (0.08)
10	327 (12.1)	0.22 (0.02)	213.0 (2.6)	0.53 (0.010)	3.35 (0.13)*
20	316 (35.7)	0.22 (0.03)	203.3 (1.5)	0.53 (0.010)	2.91 (0.42)
30	322 (6.5)	0.21 (0.01)	218.3 (0.6)	0.52 (0.004)	3.17 (0.07)
Day 2					
Control	280 (23.1)	0.16 (0.03)	198.3 (8.1)	0.54 (0.019)	2.53 (0.14)
2.5	324 (2.5)	0.12 (0.03)	212.0 (1.0)	0.52 (0.024)	2.58 (0.36)
5	324 (17.2)	0.09 (0.01)**	219.0 (4.4)*	0.49 (0.024)	2.88 (0.13)
10	285 (16.2)	0.09 (0.01)***	224.7 (5.5)*	0.48 (0.008)*	2.70 (0.01)
20	317 (55.4)	0.08 (0.01)***	224.0 (1.7)*	0.48 (0.024)*	2.83 (0.10)
30	291 (23.8)	0.08 (0.00)***	222.0 (14.8)*	0.46 (0.012)**	2.80 (0.30)
Day 3					
Control	272 (40.7)	0.10 (0.03)	224.3 (9.7)	0.46 (0.015)	1.28 (0.18)
2.5	296 (13.3)	0.07 (0.01)	227.0 (3.0)	0.46 (0.012)	1.21 (0.30)
5	291 (44.7)	0.09 (0.04)	239.7 (18.5)	0.43 (0.025)	1.30 (0.38)
10	318 (46.5)	0.07 (0.01)	258.3 (6.8)*	0.39 (0.007)***	1.58 (0.13)
20	291 (45.2)	0.07 (0.01)	252.7 (1.2)	0.40 (0.003)**	1.72 (0.37)
30	298 (37.1)	0.07 (0.01)	259.3 (15.5)*	0.38 (0.015)***	1.79 (0.27)
Day 4					
Control	327 (73.7)	0.08 (0.01)	221.3 (11.8)	0.47 (0.005)	1.85 (0.34)
2.5	295 (15.4)	0.08 (0.00)	222.0 (9.0)	0.44 (0.018)	1.85 (0.21)
5	263 (49.7)	0.08 (0.01)	216.0 (11.5)	0.38 (0.014)**	1.71 (0.18)
10	284 (93.1)	0.08 (0.00)	219.0 (7.8)	0.32 (0.006)***	2.13 (0.07)
20	338 (116.8)	0.07 (0.01)	237.3 (5.5)	0.33 (0.021)***	1.96 (0.15)
30	297 (44.4)	0.07 (0.01)	245.3 (8.0)	0.30 (0.017)***	2.22 (0.14)

2013). This resulted in the generation of amplicon sequence variants (ASVs), which were assigned taxonomy using the full-length SILVA (v138.1) reference database (Quast et al., 2012). For statistical analysis, ASV abundance and taxonomy tables were imported into R (R Core Team, 2022). Changes to community composition were visualized using relative abundance at the class level. The enrichment or depletion of abundant classes was calculated using the formula:

$$\text{Enrichment Factor (EF)} = [\text{A}]_t / [\text{A}]_c$$

where $[\text{A}]$ represents the average abundance between triplicates, c represents control Day 4, and t represents treatment (5 $\mu\text{g/L}$ – low or 30 $\mu\text{g/L}$ – high). An EF > 1 denotes enrichment, while an EF < 1 indicates depletion of the respective class in the treatment compared to the control.

2.7. Statistics

All statistical analyses were conducted in R version 4.2.2 (R Core Team, 2022). Repeated measures analysis of variance (rmANOVA) tested differences between treatments for biomass, photophysiological parameters, TEP, nutrients, and alpha diversity indices (richness, Shannon Diversity, Pielou's Evenness, and Chao1). rmANOVA's were validated using ANOVA assumptions (St and Wold, 1989); the Levene's test (homogeneity of variances) and the Shapiro-Wilks test (normality). All parameters passed these assumptions and when statistical differences ($p < 0.5$) were observed, pairwise comparisons were employed using Tukey's honestly significant difference test (Tukey HSD) (Tukey, 1949). Tukey HSD is a commonly used, robust method for parametric comparisons of equal sample sizes (Midway et al., 2020), in the context

of this work, sample sizes of $n = 3$ (triplicates) within each treatment.

Alpha and beta diversity were calculated individually for the 16S and 18S rRNA gene data using R package vegan v2.6.4 (Oksanen et al., 2022). Alpha diversity indices were calculated from the raw ASV abundance data and beta diversity using log transformed ASV abundance data to calculate Bray-Curtis dissimilarity. Bray-Curtis was visualized using a non-metric multidimensional scaling (nMDS) plot with R package ggplot2 v3.4.4 (Wickham, 2016). Differences in community composition between treatments were tested with a permutational analysis of variance (PERMANOVA, 9999 permutations) and a permutational multivariate analysis of dispersion (PERMDISP, 1000 permutations) on the Bray-Curtis dissimilarity matrix. PERMDISP is used as a multivariate extension of the Levene's test and is performed after PERMANOVA (Anderson, 2006). Standard deviation of means was calculated, and all statistical significance is reported using an alpha of 0.05.

3. Results

In situ temperature, salinity, and pH for the July (2021) and June (2023) bioassays were 28.4 °C, 24.2 ppt, and 7.96, and 27.0 °C, 36.1 ppt, and 7.80, respectively.

3.1. Biomass and photophysiological response

Comparisons in phytoplankton biomass (as chl *a*) between the PFOS and 6:2 FTS bioassays revealed that the PFOS-exposed community (1–3 $\mu\text{g/L}$) started with significantly lower biomass than the 6:2 FTS-exposed community (3–8 $\mu\text{g/L}$; $p < 2.2e-16$) (Table 1, Supplemental Table 1). General trends, though non-significant ($p > 0.05$), were observed in biomass associated with each bioassay. In PFOS-exposed communities,

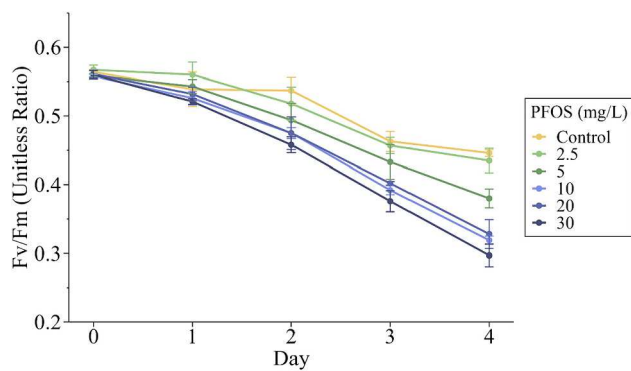


Fig. 1. PSII quantum yield (Fv/Fm) over 4 days in natural communities of phytoplankton exposed to increasing concentrations of PFOS (0, 2.5, 5, 10, 20, 30 mg/L). Error bars represent standard deviation and Fv/Fm is a unitless ratio.

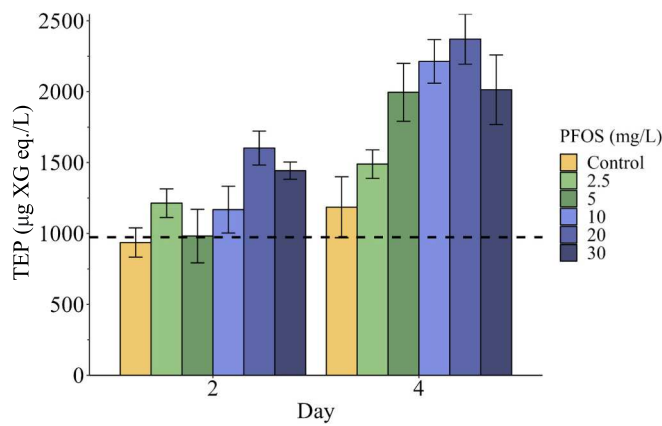


Fig. 2. Transparent exopolymer particle (TEP) abundances ($\mu\text{g XG eq./L}$) in phytoplankton communities exposed to increasing PFOS concentrations (0, 2.5, 5, 10, 20, 30 mg/L). Error bars are standard deviation, and the dashed line represents the total TEP concentration (973.72 $\mu\text{g XG eq./L}$) of control on Day 0 of the study.

biomass was generally higher compared to control from Days 1 to 4 (Table 1). In 6:2 FTS-exposed communities, biomass was generally lower from Days 3 to 4 compared to the control (Supplemental Table 1).

There were no observed differences in photophysiological parameters on Day 0 in either bioassay and PSII re-oxidation time (τ_{PSII}) was not impacted by either compound (Table 1, Supplemental Table 1). PFOS-exposed communities experienced significant differences in Fv/Fm, ρ ,

and σ_{PSII} compared to the control in a time and concentration-dependent manner (Table 1). Specifically, Fv/Fm was observed to decline in PFOS-exposed communities beginning on Days 2 and 3 of the study (Fig. 1), where treatments 10, 20, and 30 mg/L PFOS had significantly lower Fv/Fm than the control ($p > 0.05$). Subsequently, PFOS treatments of 5 mg/L to 30 mg/L on Day 4 had significantly lower Fv/Fm compared to control (0.47 ± 0.005), their PSII quantum yields as follows: 5 (0.38 ± 0.014), 10 (0.32 ± 0.006), 20 (0.33 ± 0.021), and 30 (0.29 ± 0.017) mg/L PFOS ($p < 0.01$) (Table 1). Further, on Day 2 of the study, PFOS treatments (5, 10, 20, and 30 mg/L) had significantly lowered ρ and significantly higher σ_{PSII} compared to controls ($p < 0.05$). Specific PFOS treatments (10 and 30 mg/L) had significantly higher σ_{PSII} compared to control on Day 3 of the study (Table 1). In contrast to the PFOS-exposed communities, there were few instances where 6:2 FTS-exposed communities were observed to be significantly different from the control ($p < 0.05$). These included the Fv/Fm in the 20 mg/L treatment on Day 2 and the σ_{PSII} in the 10 mg/L treatment on Day 3 (Supplemental Table 1). Given this lack of impact on biomass and photophysiology, further analysis of the 6:2 FTS bioassay was not continued.

3.2. Transparent exopolymer particles

TEP production was measured for PFOS-exposed communities and found in concentrations ranging from 936 to 2370 $\mu\text{g XG eq./L}$. In most cases, TEP release was above that of the initial community, control Day 0 (974 $\mu\text{g XG eq./L}$; Fig. 2). TEP concentration in all treatments increased over the time course. On Day 2, the 20 and 30 mg/L PFOS treatments had significantly ($p < 0.001$) higher levels of TEP than the control. On the last day of the study, all PFOS treatments had higher average TEP concentrations compared to the control and significant differences were observed in treatments from 5 to 30 mg/L PFOS ($p < 0.001$).

3.3. Dissolved nutrients

Dissolved nutrients were analyzed for PFOS treatments and observed trends varied depending on parameter (Table 2). Nitrate (NO_3^-) and nitrite (NO_2^-) concentrations were highest at the start of the experiment, $3.29 \pm 0.81 \mu\text{mol/L}$ and $1.06 \pm 0.04 \mu\text{mol/L}$, respectively, and then declined. Similarly, silica (SiO_2) concentrations declined from Days 0 to 2 but increased from Days 2 to 4 in the PFOS treatments. Phosphate (HPO_4^{2-}), ammonium (NH_4^+), and urea were highest in most PFOS treatments on Day 4 of the bioassay, though not significant ($p > 0.05$). Of the nutrient parameters, DIN:P resulted in the only significant difference between the treatments and the control (Table 2). DIN:P on Day 0 was $7.03 (\pm 0.73)$ and declined over time; all treatments were significantly

Table 2

Nutrient concentrations expressed as means in $\mu\text{mol/L}$, PFOS concentrations recorded as mg/L, and standard deviations reported in parenthesis. Significance is noted as follows, *** 0.01 and ** 0.05.

	NO_3^-	NO_2^-	NH_4^+	HPO_4^{2-}	DIN:P	Silica	Urea
<i>Day 0</i>							
Control	3.29 (0.81)	1.06 (0.04)	3.85 (0.79)	1.16 (0.12)	7.03 (0.73)	11.63 (1.19)	0.88 (0.09)
<i>Day 2</i>							
Control	0.39 (0.07)	0.25 (0.05)	3.03 (0.36)	1.31 (0.22)	2.81 (0.12)	6.50 (1.98)	0.94 (0.20)
2.5	0.36 (0.05)	0.21 (0.01)	2.77 (0.03)	1.24 (0.08)	2.72 (0.15)	5.65 (0.93)	0.84 (0.11)
5	0.42 (0.02)	0.23 (0.05)	2.98 (0.26)	1.45 (0.26)	2.53 (0.22)	5.82 (0.93)	0.93 (0.08)
10	0.37 (0.5)	0.22 (0.02)	3.10 (0.62)	1.37 (0.25)	2.69 (0.02)	5.59 (2.53)	0.80 (0.13)
20	0.36 (0.01)	0.16 (0.04)	2.64 (0.27)	1.13 (0.16)	2.80 (0.12)	3.93 (1.68)	0.69 (0.02)
30	0.44 (0.09)	0.26 (0.10)	3.05 (0.53)	1.39 (0.43)	2.76 (0.38)	6.25 (2.93)	1.06 (0.45)
<i>Day 4</i>							
Control	0.39 (0.07)	0.22 (0.05)	3.15 (0.46)	1.23 (0.19)	3.07 (0.01)	7.44 (2.28)	0.82 (0.16)
2.5	0.45 (0.02)	0.35 (0.03)	3.51 (0.26)	1.85 (0.01)	2.33 (0.17)**	10.70 (0.58)	1.09 (0.05)
5	0.59 (0.20)	0.43 (0.12)	3.65 (0.11)	1.89 (0.18)	2.48 (0.13)*	13.68 (1.42)	1.18 (0.12)
10	0.60 (0.03)	0.35 (0.02)	3.84 (0.28)	1.99 (0.00)	2.41 (0.17)*	16.61 (0.07)	1.02 (0.02)
20	0.69 (0.62)	0.35 (0.11)	4.13 (0.54)	2.05 (0.50)	2.54 (0.17)*	13.79 (5.94)	1.06 (0.32)
30	0.33 (0.08)	0.35 (0.02)	3.87 (0.15)	1.85 (0.12)	2.46 (0.16)*	14.73 (2.35)	0.91 (0.16)

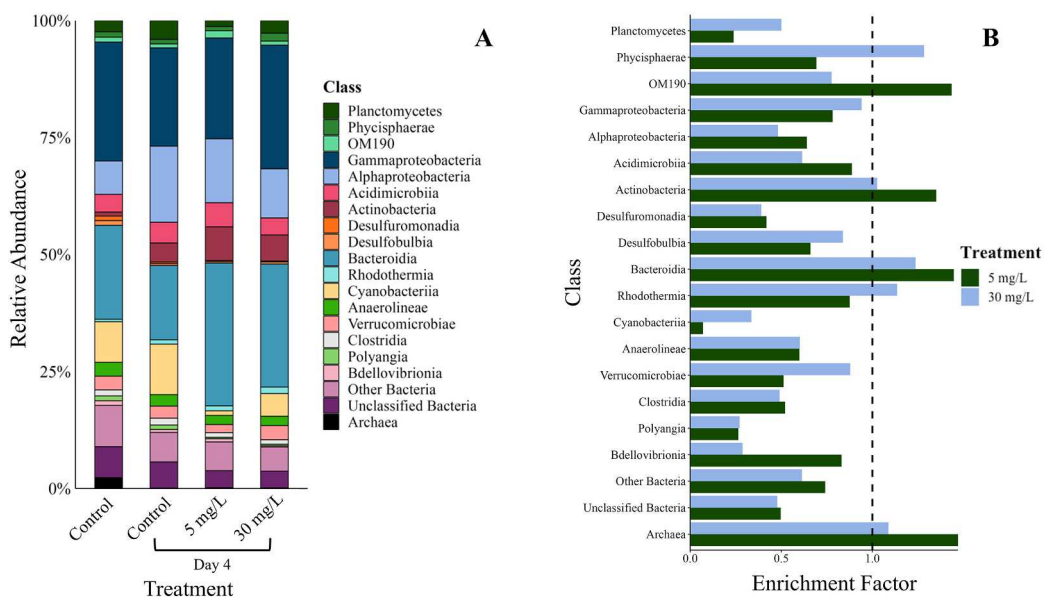


Fig. 3. (A) Prokaryotic (16S rRNA) community composition and (B) enrichment factor based on the 17 most abundant prokaryotic classes, and all ASVs classified in the following categories, “other bacteria”, “unclassified bacteria”, and “Archaea”. Enrichment factor (EF) > 1 denotes enrichment, whereas EF < 1 indicates depletion.

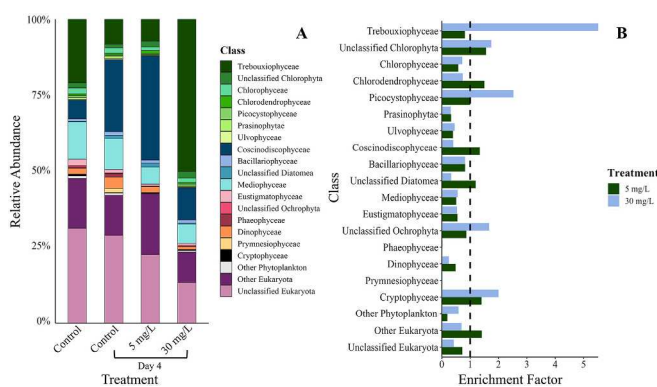


Fig. 4. (A) Eukaryotic (18S rRNA) community composition and (B) enrichment factor based on the 17 most abundant eukaryotic classes, and all ASVs classified in the following categories, “other phytoplankton”, “other eukaryota”, and “unclassified eukaryota”. Enrichment factor (EF) > 1 denotes enrichment, whereas EF < 1 indicates depletion.

Table 3

Eukaryotic and prokaryotic richness (species number and Chao1), diversity (Shannon), and evenness (Pielou). PFOS concentrations recorded as mg/L, standard deviations reported in parenthesis, and significance is noted as follows, *** 0.01 and ** 0.05.

	Number of Species	Shannon Index	Pielou's Index	Chao1
Control (Day 0)	Prokaryotic 43,599 (740)	10.34 (0.046)	0.967 (0.009)	24,576,179 (13145369)
Control (Day 4)	38,036 (7826)	10.18 (0.316)	0.966 (0.012)	18,498,503 (4377924)
5	28,991 (6760)	9.54* (0.165)	0.931** (0.007)	29,824,754 (5205301)
30	28,431 (3576)	9.76 (0.152)	0.952 (0.006)	35,200,711 (23022332)
Control (Day 0)	Eukaryotic 3200 (217)	4.594 (0.083)	0.569 (0.015)	78,489 (28806)
Control (Day 4)	2654 (244)	4.256 (0.139)	0.540 (0.019)	56,064 (24240)
5	2461 (396)	3.542** (0.204)	0.455** (0.036)	79,421 (36410)
30	2417 (488)	3.463** (0.156)	0.445** (0.020)	85,978 (27080)

Microbacteriaceae, and *Methylophagaceae*. Several families were exclusively enriched under low PFOS (*Actinomarinaceae*, *Cyclobacteriaceae*, and *OM190*), whereas *Unknown Gammaproteobacteria* were exclusively enriched under high PFOS (Supplemental Fig. 1A).

The initial control eukaryotic community (control Day 0) was dominated by members of the *Trebouxiophyceae* and *Mediophyceae* classes, making up >30 % of the community (Fig. 4). The control community shifted on Day 4, *Coscinodiscophyceae* and *Mediophyceae* dominating with percent relative abundances as follows, 23.5 % (\pm 6.21) and 10.3 % (\pm 0.08) (Supplemental Table 5). Predominant phytoplankton classes in PFOS treatments varied, the low treatment dominated by *Coscinodiscophyceae*, and the high treatment dominated by *Trebouxiophyceae*, making up 33.9 % (\pm 4.24) and 50.2 % (\pm 1.84) of the community, respectively. Enriched and depleted classes are depicted in Fig. 4B. Abundant phytoplankton families (>1 % relative abundance, on average) enriched and depleted across PFOS treatments included *Unclassified Trebouxiophyceae* and *Unclassified Chlorophyta*, and *Mediophyceae* and *Bacillariophyceae*, respectively. Two families were exclusively enriched in a single PFOS treatment, *Coscinodiscophytina* in the low and the family labelled *Incerae sedis* (class *Trebouxiophyceae*) in the high (Supplemental Fig. 1B). Notably, the majority of sequences in these families, *Coscinodiscophytina* and *Incerae sedis* (class *Trebouxiophyceae*), belonged to a single ASV of genus *Actinptychus* and *Picoclorum*, respectively.

Several alpha diversity indices were calculated for the prokaryotic and eukaryotic community: richness (number of species and Chao 1), diversity (Shannon), and evenness (Pielou) (Table 3). Higher values of each index indicate greater species richness, diversity, or evenness. The highest values for each occurred in the initial community and they declined in all treatments over time. Microbial richness was not significantly impacted by either PFOS concentration ($p > 0.05$), but diversity and evenness were. Prokaryotes declined in diversity and evenness in the low treatment, but not the high treatment (Table 3). Whereas the eukaryotic community experienced decline in both measures under each exposure. The impact on eukaryotic alpha diversity in the high treatment resulted in the lowest eukaryotic richness (2417 ± 488), diversity (3.463 ± 0.156), and evenness (0.445 ± 0.020).

Prokaryotic and eukaryotic beta diversity was visualized using nMDS; both were separated based on treatment, but prokaryotic treatments were not tightly clustered (Fig. 5A), whereas eukaryotic treatments were (Fig. 5B). PERMANOVA and PERMDISP are joint statistical

tests and were utilized to determine if this visualized separation was significant. A significant PERMANOVA indicates that there is a difference among groups, herein treatments. But a significant PERMANOVA can result from the variation between treatments or the dispersion of the triplicates. Thus, PERMDISP tested the dispersion of triplicates. Statistical tests of the prokaryotic beta diversity resulted in a significant PERMANOVA ($p < 0.05$) and PERMDISP ($p < 0.01$), therefore separation in the prokaryotic community cannot be confirmed as a result of differences between treatments but could also be caused by significant dispersion of triplicates. In contrast, eukaryotic beta diversity resulted in a significant PERMANOVA ($p = 1e-4$) and an insignificant PERMDISP ($p > 0.05$). This affirms that the eukaryotic community separation visualized on the nMDS is a result of variation between treatments.

4. Discussion

6:2 FTS was intentionally manufactured as an alternative to PFOS, but with rising concerns regarding the prevalence of PFAS substitutes in ecosystems (Field and Seow, 2017), it is essential to compare the toxicity of emerging and legacy PFAS compounds. Further, these compounds are interacting with complex microbial communities, necessitating ecosystem-relevant studies to complement previous monoculture toxicity assessments. Few studies have concomitantly compared the toxicity of unary exposures of 6:2 FTS and PFOS on microbial communities (Zhang et al., 2023a). Here, two bioassays were performed with coastal microbial communities native to the Gulf of Mexico. We found that 6:2 FTS did not elicit negative effects at the tested concentration range, but that PFOS impacted phytoplankton photosynthesis and altered stress exudate production, nutrient cycling, and the composition of the prokaryotic and eukaryotic communities.

4.1. Biomass and photophysiological response

Chl *a* concentration is commonly used as an indicator of phytoplankton cell growth (biomass) and can reveal changes in growth rates for communities exposed to PFAS. Several studies have documented that PFAS lowers chl *a* concentration in monoculture experiments (Xu et al., 2013; Muhammad et al., 2023; Zhang et al., 2023a; Zhao et al., 2023a), but Wu et al. (2022b) found that a mixture of PFAS significantly increased chl *a* in a simulated algal community. While chl *a* may be a target of PFAS toxicity, this ultimately depends on exposure time, concentration, and the PFAS compound; these factors may explain why an appreciable trend was not observed in the present study. Nonetheless, there was a significant impact on the photosynthetic apparatus, in the PFOS bioassay but not 6:2 FTS bioassay.

Photosystem II (PSII) is integral to phytoplankton photosynthesis performing the initial photosynthetic reaction, splitting water, and converting electrons into chemical energy. PSII is highly sensitive to pollutants and consequently, many studies assess changes to PSII functioning as an indicator of pollutant stress on phytoplankton photophysiology (Bretherton et al., 2019; Kamalanathan et al., 2019; Ni et al., 2023), including in PFAS assessments (Liu et al., 2022; Xue et al., 2022; Zhang et al., 2023a). Photosynthetic efficiency (Fv/Fm) indicates PSII physiological response to changing environmental conditions or stress (Suggett et al., 2009) and it was found to decline in both bioassays through time. 6:2 FTS did not elicit a significant response, which may be because it is less toxic to these communities or the concentrations tested were below levels (100 mg/L 6:2 FTS) known to lower Fv/Fm (Zhang et al., 2023a), though it should be noted that environmentally relevant concentrations are within the ng/L to ug/L range (Nguyen et al., 2019; Aly et al., 2020). In contrast, PFOS decreased photosynthetic efficiency in a concentration and time dependent manner, with higher PFOS concentrations and longer exposure resulting in lower Fv/Fm. This suggests that PFOS may target photosynthesis, eliciting phototoxicity. Recent publications corroborate (Xue et al., 2022; Zhang et al., 2023a) this finding, including at similar PFOS concentrations to those tested

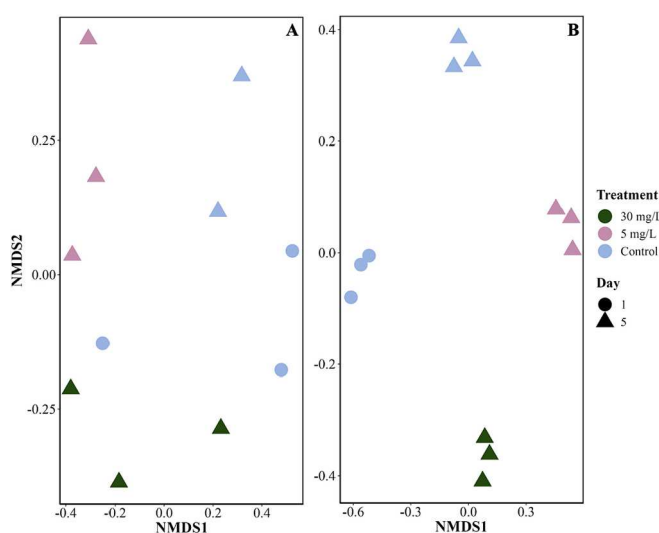


Fig. 5. nMDS of biological (A) prokaryotic and (B) eukaryotic communities. nMDS was constructed using log transformed ASV abundance data and a Bray-Curtis similarity matrix. nMDS stress for the prokaryotic and eukaryotic communities were as follows, 0.1256 and 0.0371.

here. Though photophysiological assessment of phytoplankton exposed to PFOS shows a clear inhibition of photosynthetic efficiency, the underlying mechanism remains to be determined.

To examine affected PSII processes we assessed the connectivity factor, functional absorption cross section, and re-oxidation time of PSII. 6:2 FTS was not observed to significantly alter these parameters, revealing that it did not elicit a negative effect on the Gulf of Mexico community at the concentrations used in this study. On the other hand, PFOS did alter the functioning of the photosynthetic apparatus, affecting the PSII antenna and connectivity factor. The PSII antenna captures light and converts it into excitation energy which is then transferred to an active reaction center (RC) where it undergoes three potential fates: trapping, release (e.g., heat or fluorescence), or transfer to another open RC. The connectivity factor represents the probability that captured energy is moved between PSII reaction centers rather than dissipated (Streibet, 2013). PFOS treatments (5 mg/L to 30 mg/L) significantly enlarged the antenna size and lowered the connectivity factor in the communities on Day 2. Impact to the connectivity factor suggests that PFOS lowered the probability for energy transfer between RCs, increasing the likelihood that excitation energy was released as heat or fluorescence, rather than being used for photosynthesis. Collectively, these photophysiological responses likely led to the decline in photosynthetic efficiency. Though studies have not directly measured the functional absorption cross section, PFOS and the PFAS, perfluorobutane sulfonic acid (PFBS), are known to alter the regulation of genes associated with antenna proteins (Liu et al., 2022; Xue et al., 2022), supporting the present findings. Specific PFAS, including PFOS, are also observed to effect photosynthetic efficiency and downregulate genes related to various PSII mechanisms in photosynthesizers (Li et al., 2020, 2022; Liu et al., 2022; Xue et al., 2022).

4.2. Microbial exudates

Exopolymer substances (EPS) are polysaccharide and protein rich molecules released by microbes (Santschi et al., 2021) that serve a multitude of functions, including cellular protection from toxins. Release of EPS contributes to the detoxification of xenobiotics, toxic metal ions, and reactive oxygen species thereby protecting the affected microbes (Flemming and Wingender, 2010). Transparent exopolymer particles (TEP), a type of EPS, are microgels derived from the aggregation of organic matter excreted by bacteria and phytoplankton (Passow, 2002). Release of TEP precursors is highly dependent on environmental conditions (e.g., nutrient availability, temperature) (Passow, 2002) and algal growth. TEP concentrations correlate with phytoplankton blooms (Kahl et al., 2008; Passow and Laws, 2015; Quigg et al., 2016). TEP was monitored during the PFOS bioassay, and all treatments were observed to have higher TEP concentrations on the last day of the study compared to the control. The growth of the microbial community alone did not drive higher TEP concentrations under PFOS exposure, given biomass was not significantly different between treatments. We suggest elevated TEP in PFOS treatments versus controls was a defense mechanism against the pollutant and the oxidative stress PFOS may have elicited in the communities. In situ and laboratory-based studies have shown EPS production correlates with PFOS in lake biofilms (Zhang et al., 2022) and PFOA (perfluorooctanoic acid) in green algae (Zhao et al., 2023b). These studies suggest EPS production may relieve PFAS toxicity through scavenging the tested PFAS compound, substantiated by EPS and TEP containing functional groups and proteins that may adsorb PFAS (Li et al., 2021; Yan et al., 2021). Therefore, polymeric exudates may remove PFOS from the water column and/or around microbial cells and alleviate exposure. Further studies could examine if this is a general mechanism against PFAS or a specific response to PFOS.

PFOS may have indirectly increased TEP release through inducing cellular production of reactive oxygen species (ROS) which are natural by-products of photosynthesis and other cellular functions (Pospisil, 2016). The proliferation of ROS is mediated by antioxidant enzymes

which reduce oxidative damage (Noctor and Foyer, 1998). Under environmental stressors, the antioxidant response can become overwhelmed, necessitating other mechanisms for cellular protection, including TEP secretion, which can relieve oxidative stress through physically blocking or chemically quenching ROS (Quigg et al., 2016). Specific PFAS are known to induce algal ROS production in monocultures (Xu et al., 2017; Liu et al., 2018) and simulated algal assemblages (Wu et al., 2022b). Oxidant-antioxidant disequilibrium is also widely observed under PFOS exposure, especially at higher concentrations where oxidant stress exceeds the capacity of the antioxidant systems for ROS removal (Xu et al., 2017; Xue et al., 2022; Muhammad et al., 2023). Therefore, PFOS may have increased oxidative stress leading to energy allocation for TEP production as a protective measure; expelling more exudates to quench ROS. This would need to be confirmed by assessing ROS in communities, but nevertheless, it is plausible that TEP production increased because of both PFOS and ROS pressure. This has great implications for natural ecosystems undergoing PFOS exposure as TEP is vital in carbon cycling (Passow, 2002), acts as hotspots of microbial activity (Quigg et al., 2016), and may be a driver of pollutant transport in the ocean (Santschi et al., 2021).

4.3. Prokaryotic and eukaryotic community response

The prevalent prokaryotic members present in the PFOS bioassay (Gammaproteobacteria, Bacteroidia, Cyanobacteriia, and Alphaproteobacteria) aligned well with previous literature documenting their predominance in the coastal waters of Galveston Bay, TX in the summer and when there are higher salinity (≥ 20 ppt) waters in the Gulf of Mexico coastal zone (Doyle et al., 2018, 2020; Steichen et al., 2020). It is widely reported that freshwater (O'Carroll et al., 2020; Wu et al., 2021, 2022a) and sediment (Sun et al., 2016; Bao et al., 2018; Zhang et al., 2023b) associated bacteria undergo taxonomic shifts in the presence of in situ PFAS contamination. In this study, PFOS was found to impact the community such that the class Cyanobacteriia became less dominant while the Bacteroidia and Actinobacteria classes were enriched relative to what was observed in the controls. Previous laboratory studies in which cyanobacteria were exposed to PFOS found that they were negatively impacted (Rodea-Palomares et al., 2012; Muhammad et al., 2023). But Wu et al. (2022b) found cyanobacteria may tolerate PFAS mixtures in a simulated algal-bacteria ecosystem (Wu et al., 2022b). The difference in findings could be a result of (i) testing a single compound versus a mixture, (ii) exposing a natural community versus a simulated assemblage, or (iii) the tested concentrations. Wu et al. (2022b) testing concentrations ≤ 2.6 mg/L ΣPFAS. The observed enrichment of Bacteroidia is corroborated by Cai et al. (2020), which tested PFOS on soil microbes. Further, in situ mixed contaminant studies have documented high abundance of Actinobacteria and Bacteroidia in sites associated with pollution, including PFAS contamination (Li et al., 2017; Tang et al., 2022). Our work adds to the evidence that PFAS effect prokaryotic communities of diverse ecosystems by highlighting taxonomic shifts under PFOS exposure. These taxonomic shifts may be a result of PFAS altering inter-species interactions or the ability of microbes to tolerate PFAS exposure.

The intricate relationship between bacteria and phytoplankton shapes biogeochemical cycling, particularly in response to pollution (Doyle et al., 2018, 2020; Kamalanathan et al., 2019, 2021). Therefore, PFOS altering the abundance of individuals likely had cascading effects on other microbial groups. For instance, the variation in cyanobacterial, gammaproteobacterial, and actinobacterial populations could be caused by the reported significant negative correlation between Actinobacteria and the other bacterial classes in freshwater ecosystems (Ghai et al., 2014). Specifically, the low PFOS treatment underwent greater decline in Cyanobacteriia and Gammaproteobacteria populations corresponding with increased Actinobacteria populations, specifically *Microbacteriaceae*. Further, *OM190* (Planctomycetes), which is often associated with Bacillariophyta (Pushpakumara et al., 2023), was highly

enriched in the low treatment, coinciding with higher diatom abundance. These observations should be corroborated by future studies aiming to elucidate PFAS impact to algal-bacterial interactions and assess microbial co-occurrence.

Members of *Flavobacteriaceae* (Bacteroidia), *Cyclobacteriaceae* (Bacteroidia), *Methylophagaceae* (Gammaproteobacteria), and *Microbacteriaceae* (Actinobacteria) are known to tolerate pollutant stress (e.g., polycyclic aromatic hydrocarbons) (Newton and McLellan, 2015; Remmas et al., 2017; Cerro-Gálvez et al., 2021; Lin et al., 2023). *Flavobacteriaceae* have been observed to be enriched in PFAS mixtures (PFOS and PFOA) (Cerro-Gálvez et al., 2020) and are proposed as a general biomarker for PFOA pollution (Guo et al., 2023). However, *Flavobacteriaceae* are a diverse bacterial family limiting the validity of their use as a biomarker, and their enrichment may be confounded with increases in TEP. *Flavobacteriaceae* are often associated with TEP (Taylor and Cunliffe, 2017; Zäncker et al., 2018), and along with the other enriched bacterial families (*Cyclobacteriaceae*, *Methylophagaceae*, and *Microbacteriaceae*), can degrade polysaccharides (Buchan et al., 2014; Pinnaka and Tanuku, 2014; Yeager et al., 2017; Francis et al., 2021). The survival of members within each family could then be attributed to their ability to use TEP-derived polysaccharides for growth. Therefore, the observed taxonomic shifts may not be a direct result of interactions with PFOS, but rather an indirect result connected to TEP-induced processes. Nonetheless, these results provide insight for identifying PFOS tolerant bacterial members. Further, our observations of lowered evenness and diversity in the low treatment group, connect to previous studies that documented variations in alpha diversity in response to in situ PFAS levels (Sun et al., 2016; Bao et al., 2018; Zhang et al., 2023b). Our findings reveal PFOS affects diversity measures and composition of prokaryotic communities, but notably the low treatment underwent greater impact. Considering previous work, these alterations may also be controlled by the PFAS compound or concentration, in addition to the physicochemical parameters of the studied ecosystem.

A paucity of information exists regarding PFAS impact on natural phytoplankton communities. Further, marine algae have been largely excluded in the literature evaluating PFAS toxicity on phytoplankton in culture studies. Instead, the literature widely documents the response of freshwater species of green algae (Boudreau et al., 2003; Liu et al., 2008, 2009; Xu et al., 2017; Xue et al., 2022) or cyanobacteria (Rodea-Palomares et al., 2012; Muhammad et al., 2023). These studies have provided invaluable information and formed the foundation for scientific knowledge of algal-PFAS interactions, yet there is a potential that marine and freshwater species differ in response to PFAS. Our findings indicate that marine algae composition changes in a concentration-dependent manner, with more tolerant species displacing sensitive species when comparing the low and high treatments. Specifically, diatoms (*Coscinodiscophyceae*), dominating the low treatment, were replaced by green algae (*Trebouxiophyceae* and *Chlorophyta*) in the high treatment. The resilience of diatoms and green algae in their respective treatments is not surprising, as these groups are generally documented to tolerate pollutant exposures (e.g., crude oil) (Quigg et al., 2021) and recover after environmental hazards (e.g., hurricanes) (Steichen et al., 2020) compared to cyanobacteria and dinoflagellates.

At a finer taxonomic level, we observed algal tolerance as family dependent, specific diatom and green algae enriched, while others were depleted. Regarding the low treatment, *Coscinodiscophytina* overcame PFOS stress, but *Mediophyceae* and *Bacillariophyceae* were depleted across treatments, suggesting not all diatoms can withstand PFOS exposure. The observed robust nature of *Coscinodiscophytina* cannot be explained by general characteristics alone, *Mediophyceae* and *Coscinodiscophytina* both centric diatom families with no known differentiation in size class. Therefore, *Coscinodiscophytina*, particularly the genus *Actinptychus*, may have adaptive strategies to deal with PFOS exposure, but with limited information on diatom-PFAS interactions, this cannot be determined and should be a focus in future work. In the high treatment, *Incetae sedis* (class *Trebouxiophyceae*), *Unclassified*

Trebouxiophyceae, and *Unclassified Chlorophyta* were enriched. This corresponds to findings by Wu et al. (2022b) who documented higher relative abundances of *Trebouxiophyceae* (>70 %) in all PFAS treatments after 3 days while *Chlorophyta* showed strong PFAS tolerance, and *Bacillariophyta* appeared vulnerable to PFAS (Wu et al., 2022b). Further, we documented that the majority of *Incetae sedis* (class *Trebouxiophyceae*) sequences belonged to the ASV of genus *Picochlorum*, which has been described as a polyextremotolerant algae that quickly adapts to changing environmental conditions (Foflonker et al., 2016). Notably, our findings suggest that there are green algae and diatoms that can tolerate the tested PFOS concentrations, and we reveal algal classes and families that are vulnerable to PFOS exposure. Additionally, we report that eukaryotic diversity and evenness decline with increasing PFOS concentration and that eukaryotic communities were distinctly different between treatments. This contrasted the prokaryotic findings and reveals that eukaryotic populations were more vulnerable to PFOS than prokaryotic communities.

Aquatic microbes are integral to ecosystem stability. Therefore, investigating microbial response to pollutant exposure is pertinent in synthesizing whole-system effects. This study investigated the impact (photophysiological response, exudate production, nutrient cycling, and disruption to community composition) of two PFAS, PFOS or 6:2 FTS, on coastal microbial communities. 6:2 FTS was not observed to impact biomass or photophysiology, whereas PFOS did. This highlights that 6:2 FTS may be a safer alternative to PFOS when considering microbial communities exposed to the concentrations tested here. On the other hand, PFOS elicited phototoxicity, stimulated TEP production, and altered the composition and diversity of the microbial community, impacting eukaryotes more than prokaryotes. An important consideration from this work is that the microbial response to PFOS may be dependent on the initial community composition and the sampling location. It is possible that microbial communities adjacent to locations in which PFAS are purposely or accidentally released, e.g., industrial complexes or the use of aqueous film forming foams, may differ in their response. While this study provides important insights for understanding how PFAS will impact aquatic ecosystems, future work should investigate PFAS on a broader range of native assemblages with the aim to identify consistent biomarkers of microbial response.

CRediT authorship contribution statement

Sarah N. Davis: Writing – review & editing, Writing – original draft, Visualization, Methodology, Investigation, Formal analysis, Data curation, Conceptualization. **Shaley M. Klumker:** Writing – review & editing, Investigation, Data curation, Conceptualization. **Alexis A. Mitchell:** Investigation, Data curation. **Marshall A. Coppage:** Investigation, Data curation. **Jessica M. Labonté:** Writing – review & editing, Methodology, Formal analysis. **Antonietta Quigg:** Writing – review & editing, Resources, Methodology, Funding acquisition, Conceptualization.

Declaration of competing interest

The authors declare that they have no known competing financial interests or personal relationships that could have appeared to influence the work reported in this paper.

Data availability

Data will be made available on request.

Acknowledgement

This material is based totally or in part upon work supported by the National Science Foundation Rapid Response Research Grant No. HDBE-1936174 to Hala; and Research and Development program of the Texas

General Land Office Oil Spill Prevention and Response Division under Grant No. 20-057-000-B908 to Quigg. We would like to thank all members of the Phytoplankton Dynamics lab at Texas A&M University at Galveston (TAMUG) that assisted with sample collection and processing, including students from the Ocean and Coastal Research Experiences for Undergraduates (OCEANUS) program hosted by TAMUG. Rayna Nolen, David Hala and Karl Kasier at TAMUG supported development of the PFAS protocols. S.M.K and A.A.M were supported by ACES scholarships from TAMUG. M.A.C was supported by an NSF REU OCEANUS (Award#1950910) fellowship. We acknowledge that the graphical abstract of this work was created with [BioRender.com](https://biorender.com). We thank the three anonymous reviewer's and the editor for their comments and recommendations which improved our manuscript.

Appendix A. Supplementary data

Supplementary data to this article can be found online at <https://doi.org/10.1016/j.scitotenv.2024.171977>.

References

Ahrens, L., Bundschuh, M., 2014. Fate and effects of poly- and perfluoroalkyl substances in the aquatic environment: a review. *Environ. Toxicol. Chem.* 33, 1921–1929. <https://doi.org/10.1002/etc.2663>.

Aly, N.A., Luo, Y.-S., Liu, Y., Casillas, G., McDonald, T.J., Kaihatu, J.M., et al., 2020. Temporal and spatial analysis of per and polyfluoroalkyl substances in surface waters of Houston ship channel following a large-scale industrial fire incident. *Environ. Pollut.* 265, 115009. <https://doi.org/10.1016/j.envpol.2020.115009>.

Anderson, M.J., 2006. Distance-based tests for homogeneity of multivariate dispersions. *Biometrics* 62, 245–253. <https://doi.org/10.1111/j.1541-0420.2005.00440.x>.

Arar, E., Collins, G., 1997. *Method 445.0: In Vitro Determination of Chlorophyll a and Pheophytin a in Marine and Freshwater Algae by Fluorescence*. National Exposure Research Laboratory: U.S. Environmental Protection Agency.

Bao, Y., Li, B., Xie, S., Huang, J., 2018. Vertical profiles of microbial communities in perfluoroalkyl substance-contaminated soils. *Ann. Microbiol.* 68, 399–408. <https://doi.org/10.1007/s13213-018-1346-y>.

Beach, S.A., Newsted, J.L., Coady, K., Giesy, J.P., 2006. Ecotoxicological evaluation of perfluorooctanesulfonate (PFOS). *Rev. Environ. Contam. Toxicol.* 133–174 https://doi.org/10.1007/0-387-32883-1_5.

Bérard, A., 1996. Effect of organic four solvents on natural phytoplankton assemblages: consequences for ecotoxicological experiments on herbicides. *Bull. Environ. Contam. Toxicol.* 57, 183–190. <https://doi.org/10.1007/s001289900173>.

Bittar, T.B., Passow, U., Hamaraty, L., Bidle, K.D., Harvey, E.L., 2018. An updated method for the calibration of transparent exopolymer particle measurements. *Limnol. Oceanogr. Methods* 16 (10), 621–628. <https://doi.org/10.1002/lom.310268>.

Boudreau, T.M., Sibley, P.K., Mabury, S.A., Muir, D.G.C., Solomon, K.R., 2003. Laboratory evaluation of the toxicity of perfluorooctane sulfonate (PFOS) on *Selenastrum capricornutum*, *Chlorella vulgaris*, *Lemna gibba*, *Daphnia magna*, and *Daphnia pulicaria*. *Arch. Environ. Contam. Toxicol.* 44, 307–313. <https://doi.org/10.1007/s00244-002-2102-6>.

Bradley, I.M., Pinto, A.J., Guest, J.S., 2016. Design and evaluation of Illumina MiSeq-compatible, 18S rRNA gene-specific primers for improved characterization of mixed phototrophic communities. *Appl. Environ. Microbiol.* 82, 5878–5891. <https://doi.org/10.1128/AEM.01630-16>.

Bretherton, L., Kamalanathan, M., Genzer, J., Hillhouse, J., Setta, S., Liang, Y., et al., 2019. Response of natural phytoplankton communities exposed to crude oil and chemical dispersants during a mesocosm experiment. *Aquat. Toxicol.* 206, 43–53. <https://doi.org/10.1016/j.aquatox.2018.11.004>.

Buchan, A., LeCleir, G.R., Gulvik, C.A., González, J.M., 2014. Master recyclers: features and functions of bacteria associated with phytoplankton blooms. *Nat. Rev. Microbiol.* 12, 686–698. <https://doi.org/10.1038/nrmicro3326>.

Cai, Y., Chen, H., Yuan, R., Wang, F., Chen, Z., Zhou, B., 2020. Metagenomic analysis of soil microbial community under PFOA and PFOS stress. *Environ. Res.* 188, 109838 <https://doi.org/10.1016/j.envres.2020.109838>.

Caporaso, J.G., Lauber, C.L., Walters, W.A., Berg-Lyons, D., Lozupone, C.A., Turnbaugh, P.J., et al., 2011. Global patterns of 16S rRNA diversity at a depth of millions of sequences per sample. *Proc. Natl. Acad. Sci.* 108, 4516–4522. <https://doi.org/10.1073/pnas.1000080107>.

Casal, P., González-Gaya, B., Zhang, Y., Reardon, A.J.F., Martin, J.W., Jiménez, B., et al., 2017. Accumulation of perfluoroalkylated substances in oceanic plankton. *Environ. Sci. Technol.* 51, 2766–2775. <https://doi.org/10.1021/acs.est.6b05821>.

Cerro-Gálvez, E., Roscales, J.L., Jiménez, B., Sala, M.M., Dachs, J., Vila-Costa, M., 2020. Microbial responses to perfluoroalkyl substances and perfluorooctanesulfonate (PFOS) desulfurization in the Antarctic marine environment. *Water Res.* 171, 115434 <https://doi.org/10.1016/j.watres.2019.115434>.

Cerro-Gálvez, E., Dachs, J., Lundin, D., Fernández-Pinos, M.-C., Sebastián, M., Vila-Costa, M., 2021. Responses of coastal marine microbiomes exposed to anthropogenic dissolved organic carbon. *Environ. Sci. Technol.* 55, 9609–9621. <https://doi.org/10.1021/acs.est.0c07262>.

Chassot, E., Mélin, F., Le Pape, O., Gascuel, D., 2007. Bottom-up control regulates fisheries production at the scale of eco-regions in European seas. *Mar. Ecol. Prog. Ser.* 343, 45–55. <https://doi.org/10.3354/meps06919>.

Cheng, H., Jin, H., Lu, B., Lv, C., Ji, Y., Zhang, H., et al., 2023. Emerging poly- and perfluoroalkyl substances in water and sediment from Qiantang River-Hangzhou Bay. *Sci. Total Environ.* 875, 162687 <https://doi.org/10.1016/j.scitotenv.2023.162687>.

Coggan, T.L., Moodie, D., Kolobaric, A., Szabo, D., Shimeta, J., Crosbie, N.D., et al., 2019. An investigation into per- and polyfluoroalkyl substances (PFAS) in nineteen Australian wastewater treatment plants (WWTPs). *Heliyon* 5, e02316. <https://doi.org/10.1016/j.heliyon.2019.e02316>.

Conder, J.M., Hoke, R.A., Wolf, W.D., Russell, M.H., Buck, R.C., 2008. Are PFCAs bioaccumulative? A critical review and comparison with regulatory criteria and persistent lipophilic compounds. *Environ. Sci. Technol.* 42, 995–1003. <https://doi.org/10.1021/es070895g>.

Cotner, J.B., Biddanda, B.A., 2002. Small players, large role: microbial influence on biogeochemical processes in pelagic aquatic ecosystems. *Ecosystems* 5, 105–121. <https://doi.org/10.1007/s10021-001-0059-3>.

Doyle, S.M., Whitaker, E.A., De Pascuale, V., Wade, T.L., Knap, A.H., Santschi, P.H., et al., 2018. Rapid formation of microbe-oil aggregates and changes in community composition in coastal surface water following exposure to oil and the dispersant Corexit. *Front. Microbiol.* 9, 689. <https://doi.org/10.3389/fmicb.2018.00689>.

Doyle, S.M., Lin, G., Morales-McDevitt, M., Wade, T.L., Quigg, A., Sylvan, J.B., 2020. Niche partitioning between coastal and offshore shelf waters results in differential expression of alkane and polycyclic aromatic hydrocarbon catabolic pathways. *mSystems* 5, e00668-20. <https://doi.org/10.1128/mSystems.00668-20>.

Field, J.A., Seow, J., 2017. Properties, occurrence, and fate of fluorotelomer sulfonates. *Crit. Rev. Environ. Sci. Technol.* 47, 643–691. <https://doi.org/10.1080/10643389.2017.1326276>.

Fitzgerald, N.J.M., Wargenaan, A., Sorenson, C., Pedersen, J., Tufenkji, N., Novak, P.J., et al., 2018. Partitioning and accumulation of perfluoroalkyl substances in model lipid bilayers and bacteria. *Environ. Sci. Technol.* 52, 10433–10440. <https://doi.org/10.1021/acs.est.8b02912>.

Flemming, H.-C., Wingender, J., 2010. The biofilm matrix. *Nat. Rev. Microbiol.* 8, 623–633. <https://doi.org/10.1038/nrmicro2415>.

Foflonker, F., Ananyev, G., Qiu, H., Morrison, A., Palenik, B., Dismukes, G.C., et al., 2016. The unexpected extremophile: tolerance to fluctuating salinity in the green alga *Picochlorum*. *Algal Res.* 16, 465–472. <https://doi.org/10.1016/j.algal.2016.04.003>.

Francis, B., Urich, T., Mikolasch, A., Teeling, H., Amann, R., 2021. North Sea spring bloom-associated Gammaproteobacteria fill diverse heterotrophic niches. *Environ. Microbiome* 16, 15. <https://doi.org/10.1186/s40793-021-00385-y>.

Gaines, L.G.T., Sinclair, G., Williams, A.J., 2023. A proposed approach to defining per- and polyfluoroalkyl substances (PFAS) based on molecular structure and formula. *Integr. Environ. Assess. Manag.* iem.4735 <https://doi.org/10.1002/ieam.4735>.

Ghai, R., Mizuno, C.M., Picazo, A., Camacho, A., Rodriguez-Valera, F., 2014. Key roles for freshwater Actinobacteria revealed by deep metagenomic sequencing. *Mol. Ecol.* 23, 6073–6090. <https://doi.org/10.1111/mec.12985>.

Guo, C., Ahrens, L., Bertilsson, S., Coolen, M.J.L., Tang, J., 2023. Microcosm experiment to test bacterial responses to perfluorooctanoate exposure. *Sci. Total Environ.* 857, 159685 <https://doi.org/10.1016/j.scitotenv.2022.159685>.

Hoke, R.A., Ferrell, B.D., Ryan, T., Sloman, T.L., Green, J.W., Nabb, D.L., et al., 2015. Aquatic hazard, bioaccumulation and screening risk assessment for 6:2 fluorotelomer sulfonate. *Chemosphere* 128, 258–265. <https://doi.org/10.1016/j.chemosphere.2015.01.033>.

Huot, Y., Babin, M., Bruyant, F., Grob, C., Twardowski, M.S., Claustre, H., 2007. Does chlorophyll a provide the best index of phytoplankton biomass for primary productivity studies? *Biogeosci. Discuss.* 4 (2), 707–745. <https://doi.org/10.5194/bgd-4-707-2007>.

Kahl, L., Vardi, A., Schofield, O., 2008. Effects of phytoplankton physiology on export flux. *Mar. Ecol. Prog. Ser.* 354, 3–19. <https://doi.org/10.3354/meps07333>.

Kamalanathan, M., Chiu, M.-H., Bacosa, H., Schwehr, K., Tsai, S.-M., Doyle, S., et al., 2019. Role of polysaccharides in diatom *Thalassiosira pseudonana* and its associated bacteria in hydrocarbon presence. *Plant Physiol.* 180, 1898–1911. <https://doi.org/10.1104/pp.19.00301>.

Kamalanathan, M., Schwehr, K.A., Labonté, J.M., Taylor, C., Bergen, C., Patterson, N., et al., 2021. The interplay of phototrophic and heterotrophic microbes under oil exposure: a microcosm study. *Front. Microbiol.* 12, 675328 <https://doi.org/10.3389/fmicb.2021.675328>.

Kolber, Z.S., Prášil, O., Falkowski, P.G., 1998. Measurements of variable chlorophyll fluorescence using fast repetition rate techniques: defining methodology and experimental protocols. *Biochim. Biophys. Acta Bioenergetics* 1367, 88–106. [https://doi.org/10.1016/S0005-2728\(98\)00135-2](https://doi.org/10.1016/S0005-2728(98)00135-2).

Kozich, J.J., Westcott, S.L., Baxter, N.T., Highlander, S.K., Schloss, P.D., 2013. Development of a dual-index sequencing strategy and curation pipeline for analyzing amplicon sequence data on the MiSeq illumina sequencing platform. *Appl. Environ. Microbiol.* 79, 5112–5120. <https://doi.org/10.1128/AEM.01043-13>.

Krupa, P.M., Lotufo, G.R., Mylroie, E.J., May, L.K., Gust, K.A., Kimble, A.N., et al., 2022. Chronic aquatic toxicity of perfluorooctane sulfonic acid (PFOS) to Ceriodaphnia dubia, Chironomus dilutus, Danio rerio, and Hyalella azteca. *Ecotoxicol. Environ. Saf.* 241, 113838 <https://doi.org/10.1016/j.ecoenv.2022.113838>.

Lam, N.-H., Cho, C.-R., Lee, J.-S., Soh, H.-Y., Lee, B.-C., Lee, J.-A., et al., 2014. Perfluorinated alkyl substances in water, sediment, plankton and fish from Korean rivers and lakes: a nationwide survey. *Sci. Total Environ.* 491–492, 154–162. <https://doi.org/10.1016/j.scitotenv.2014.01.045>.

Li, B., Bao, Y., Xu, Y., Xie, S., Huang, J., 2017. Vertical distribution of microbial communities in soils contaminated by chromium and perfluoroalkyl substances. *Sci. Total Environ.* 599–600, 156–164. <https://doi.org/10.1016/j.scitotenv.2017.04.241>.

Li, R., Tang, T., Qiao, W., Huang, J., 2020. Toxic effect of perfluorooctane sulfonate on plants in vertical-flow constructed wetlands. *J. Environ. Sci.* 92, 176–186. <https://doi.org/10.1016/j.jes.2020.02.018>.

Li, X., Hua, Z., Wu, J., Gu, L., 2021. Removal of perfluoroalkyl acids (PFAAs) in constructed wetlands: considerable contributions of submerged macrophytes and the microbial community. *Water Res.* 197, 117080 <https://doi.org/10.1016/j.watres.2021.117080>.

Li, J., Sun, J., Li, P., 2022. Exposure routes, bioaccumulation and toxic effects of per- and polyfluoroalkyl substances (PFASs) on plants: a critical review. *Environ. Int.* 158, 106891 <https://doi.org/10.1016/j.envint.2021.106891>.

Lim, J., 2022. Broad toxicological effects of per-/poly- fluorooalkyl substances (PFAS) on the unicellular eukaryote, *Tetrahymena pyriformis*. *Environ. Toxicol. Pharmacol.* 95, 103954 <https://doi.org/10.1016/j.etap.2022.103954>.

Lin, W., Fan, F., Xu, G., Gong, K., Cheng, X., Yuan, X., et al., 2023. Microbial community assembly responses to polycyclic aromatic hydrocarbon contamination across water and sediment habitats in the Pearl River Estuary. *J. Hazard. Mater.* 457, 131762 <https://doi.org/10.1016/j.jhazmat.2023.131762>.

Litchman, E., Tezanos Pinto, P., Edwards, K.F., Klausmeier, C.A., Kremer, C.T., Thomas, M.K., 2015. Global biogeochemical impacts of phytoplankton: a trait-based perspective. *J. Ecol.* 103, 1384–1396. <https://doi.org/10.1111/1365-2745.12438>.

Liu, W., Chen, S., Quan, X., Jin, Y.-H., 2008. Toxic effect of serial perfluorosulfonic and perfluorocarboxylic acids on the membrane system of a freshwater alga measured by flow cytometry. *Environ. Toxicol. Chem.* 27, 1597. <https://doi.org/10.1897/07-459.1>.

Liu, W., Zhang, Y.-B., Quan, X., Jin, Y.-H., Chen, S., 2009. Effect of perfluorooctane sulfonate on toxicity and cell uptake of other compounds with different hydrophobicity in green alga. *Chemosphere* 75, 405–409. <https://doi.org/10.1016/j.chemosphere.2008.11.084>.

Liu, G., Zhang, S., Yang, K., Zhu, L., Lin, D., 2016. Toxicity of perfluorooctane sulfonate and perfluorooctanoic acid to *Escherichia coli*: membrane disruption, oxidative stress, and DNA damage induced cell inactivation and/or death. *Environ. Pollut.* 214, 806–815. <https://doi.org/10.1016/j.envpol.2016.04.089>.

Liu, W., Li, J., Gao, L., Zhang, Z., Zhao, J., He, X., et al., 2018. Bioaccumulation and effects of novel chlorinated polyfluorinated ether sulfonate in freshwater alga *Scenedesmus obliquus*. *Environ. Pollut.* 233, 8–15. <https://doi.org/10.1016/j.envpol.2017.10.039>.

Liu, X., Zheng, X., Zhang, L., Li, J., Li, Y., Huang, H., et al., 2022. Joint toxicity mechanisms of binary emerging PFAS mixture on algae (*Chlorella pyrenoidosa*) at environmental concentration. *J. Hazard. Mater.* 437, 129355 <https://doi.org/10.1016/j.jhazmat.2022.129355>.

Ma, T., Wu, P., Wang, L., Li, Q., Li, X., Luo, Y., 2023. Toxicity of per- and polyfluoroalkyl substances to aquatic vertebrates. *Front. Environ. Sci.* 11, 1101100 <https://doi.org/10.3389/fenvs.2023.1101100>.

Masoner, J.R., Kolpin, D.W., Cozzarelli, I.M., Smalling, K.L., Bolyard, S.C., Field, J.A., et al., 2020. Landfill leachate contributes per-/poly-fluoroalkyl substances (PFAS) and pharmaceuticals to municipal wastewater. *Environ. Sci.: Water Res. Technol.* 6, 1300–1311. <https://doi.org/10.1039/DOW00045K>.

Midway, S., Robertson, M., Flinn, S., Kaller, M., 2020. Comparing multiple comparisons: practical guidance for choosing the best multiple comparisons test. *PeerJ* 8, e10387. <https://doi.org/10.7717/peerj.10387>.

Moore, C.M., Mills, M.M., Langlois, R., Milne, A., Achterberg, E.P., La Roche, J., et al., 2008. Relative influence of nitrogen and phosphorous availability on phytoplankton physiology and productivity in the oligotrophic sub-tropical North Atlantic Ocean. *Limnol. Oceanogr.* 53, 291–305. <https://doi.org/10.4319/lo.2008.53.1.0291>.

Muhammad, F.S., Chia, M.A., Abolude, D.S., Tamizu, S., Otoogo, R.A., 2023. Growth, antioxidant response and microcystin production by *Microcystis aeruginosa* exposed to the surfactant perfluorooctanesulfonic acid (PFOS). *Phycologia* 62, 259–267. <https://doi.org/10.1080/00318884.2023.2189408>.

Muir, D., Miaz, L.T., 2021. Spatial and temporal trends of perfluoroalkyl substances in global ocean and coastal waters. *Environ. Sci. Technol.* 55, 9527–9537. <https://doi.org/10.1021/acs.est.0c08035>.

Naile, J.E., Khim, J.S., Wang, T., Chen, C., Luo, W., Kwon, B.-O., et al., 2010. Perfluorinated compounds in water, sediment, soil and biota from estuarine and coastal areas of Korea. *Environ. Pollut.* 158, 1237–1244. <https://doi.org/10.1016/j.envpol.2010.01.023>.

Newton, R.J., McLellan, S.L., 2015. A unique assemblage of cosmopolitan freshwater bacteria and higher community diversity differentiate an urbanized estuary from oligotrophic Lake Michigan. *Front. Microbiol.* 6 <https://doi.org/10.3389/fmicb.2015.01028>.

Nguyen, H.T., Kaserzon, S.L., Thai, P.K., Vijayasarathy, S., Bräunig, J., Crosbie, N.D., et al., 2019. Temporal trends of per- and polyfluoroalkyl substances (PFAS) in the influent of two of the largest wastewater treatment plants in Australia. *Emerg. Contam.* 5, 211–218. <https://doi.org/10.1016/j.emcon.2019.05.006>.

Ni, Z., Tan, L., Wang, J., Chen, Y., Zhang, N., Meng, F., et al., 2023. Toxic effects of pristine and aged polystyrene and their leachate on marine microalgae *Skeletonema costatum*. *Sci. Total Environ.* 857, 159614 <https://doi.org/10.1016/j.scitotenv.2022.159614>.

Noctor, G., Foyer, C.H., 1998. Ascorbate and glutathione: keeping active oxygen under control. *Annu. Rev. Plant. Physiol. Plant. Mol. Biol.* 49, 249–279. <https://doi.org/10.1146/annurev.aplant.49.1.249>.

Nolen, R.M., Faulkner, P., Ross, A.D., Kaiser, K., Quigg, A., Hala, D., 2022. PFASs pollution in Galveston Bay surface waters and biota (shellfish and fish) following AFFFs use during the ITC fire at Deer Park (March 17th–20th 2019), Houston, TX. *Sci. Total Environ.* 805, 150361 <https://doi.org/10.1016/j.scitotenv.2021.150361>.

Nolen, R.M., Prouse, A., Russell, M.L., Bloodgood, J., Díaz Clark, C., Carmichael, R.H., et al., 2024. Evaluation of fatty acids and carnitine as biomarkers of PFOS exposure in biota (fish and dolphin) from Galveston Bay and the northwestern Gulf of Mexico. *Comp. Biochem. Physiol., Part C: Toxicol. Pharmacol.* 276, 109817 <https://doi.org/10.1016/j.cbpc.2023.109817>.

Novak, P.A., Hoeksema, S.D., Thompson, S.N., Trayler, K.M., 2023. Per- and polyfluoroalkyl substances (PFAS) contamination in a microtidal urban estuary: sources and sinks. *Mar. Pollut. Bull.* 193, 115215 <https://doi.org/10.1016/j.marpolbul.2023.115215>.

O'Carroll, D.M., Jeffries, T.C., Lee, M.J., Le, S.T., Yeung, A., Wallace, S., et al., 2020. Developing a roadmap to determine per- and polyfluoroalkyl substances-microbial population interactions. *Sci. Total Environ.* 712, 135994 <https://doi.org/10.1016/j.scitotenv.2019.135994>.

Oksanen, J., Simpson, G., Blanchet, F., Kindt, R., Legendre, P., Minchin, P., et al., 2022. vegan: community ecology package. Available at: <https://CRAN.R-project.org/package=vegan>.

Passow, U., 2002. Transparent exopolymer particles (TEP) in aquatic environments. *Prog. Oceanogr.* 55, 287–333. [https://doi.org/10.1016/S0079-6610\(02\)00138-6](https://doi.org/10.1016/S0079-6610(02)00138-6).

Passow, U., Alldredge, A.L., 1995. A dye-binding assay for the spectrophotometric measurement of transparent exopolymer particles (TEP). *Limnol. Oceanogr.* 40 (7), 1326–1335. <https://doi.org/10.4319/lo.1995.40.7.1326>.

Passow, U., Laws, E., 2015. Ocean acidification as one of multiple stressors: growth response of *Thalassiosira weissflogii* (diatom) under temperature and light stress. *Mar. Ecol. Prog. Ser.* 541, 75–90. <https://doi.org/10.3354/meps11541>.

Pinnaka, A.K., Tanuku, N.R.S., 2014. The Family Cyclocladaceae. Springer-Verlag, Berlin. https://doi.org/10.1007/978-3-642-38954-2_139.

Podder, A., Sadmani, A.H.M.A., Reinhart, D., Chang, N.-B., Goel, R., 2021. Per and polyfluoroalkyl substances (PFAS) as a contaminant of emerging concern in surface water: a transboundary review of their occurrences and toxicity effects. *J. Hazard. Mater.* 419, 126361 <https://doi.org/10.1016/j.jhazmat.2021.126361>.

Pospíšil, P., 2016. Production of reactive oxygen species by photosystem II as a response to light and temperature stress. *Front. Plant Sci.* 7 <https://doi.org/10.3389/fpls.2016.01950>.

Prevedouros, K., Cousins, I.T., Buck, R.C., Korzeniowski, S.H., 2006. Sources, fate and transport of perfluorocarboxylates. *Environ. Sci. Technol.* 40, 32–44. <https://doi.org/10.1021/es0512475>.

Pushpakumara, B.L.D.U., Tandon, K., Willis, A., Verbruggen, H., 2023. Unravelling microalgal-bacterial interactions in aquatic ecosystems through 16S rRNA gene-based co-occurrence networks. *Sci. Rep.* 13, 2743. <https://doi.org/10.1038/s41598-023-27816-9>.

Qiao, W., Xie, Z., Zhang, Y., Liu, X., Xie, S., Huang, J., Yu, L., 2018. Perfluoroalkyl substances (PFASs) influence the structure and function of soil bacterial community: greenhouse experiment. *Sci. Total Environ.* 642, 1118–1126. <https://doi.org/10.1016/j.scitotenv.2018.06.113>.

Quast, C., Pruesse, E., Yilmaz, P., Gerken, J., Schweer, T., Yarza, P., et al., 2012. The SILVA ribosomal RNA gene database project: improved data processing and web-based tools. *Nucleic Acids Res.* 41, D590–D596. <https://doi.org/10.1093/nar/gks1219>.

Quigg, A., Sylvan, J.B., Gustafson, A.B., Fisher, T.R., Oliver, R.L., Tozzi, S., et al., 2011. Going west: nutrient limitation of primary production in the Northern Gulf of Mexico and the importance of the Atchafalaya River. *Aquat. Geochem.* 17, 519–544. <https://doi.org/10.1007/s10498-011-9134-3>.

Quigg, A., Passow, U., Chin, W., Xu, C., Doyle, S., Bretherton, L., et al., 2016. The role of microbial exopolymers in determining the fate of oil and chemical dispersants in the ocean. *Limnol. Oceanogr. Lett.* 1, 3–26. <https://doi.org/10.1002/lo2.10030>.

Quigg, A., Parsons, M., Bargu, S., Ozhan, K., Daly, K.L., Chakraborty, S., et al., 2021. Marine phytoplankton responses to oil and dispersant exposures: knowledge gained since the deepwater horizon oil spill. *Mar. Pollut. Bull.* 164, 112074 <https://doi.org/10.1016/j.marpolbul.2021.112074>.

R Core Team, 2022. R: A language and environment for statistical computing. Available at: <https://www.R-project.org/>.

Ramírez-Canon, A., Paola Becerra-Quiroz, A., Herrera-Jacuelin, F., 2022. Perfluoroalkyl and polyfluoroalkyl substances (PFAS): first survey in water samples from the Bogotá River, Colombia. *Environ. Adv.* 8, 100223 <https://doi.org/10.1016/j.envadv.2022.100223>.

Rankin, K., Mabury, S.A., Jenkins, T.M., Washington, J.W., 2016. A North American and global survey of perfluoroalkyl substances in surface soils: distribution patterns and mode of occurrence. *Chemosphere* 161, 333–341. <https://doi.org/10.1016/j.chemosphere.2016.06.109>.

Remmas, N., Melidis, P., Voltsi, C., Athanasiou, D., Ntougias, S., 2017. Novel hydrolytic extremely halotolerant alkaliphiles from mature landfill leachate with key involvement in maturation process. *J. Environ. Sci. Health A* 52, 64–73. <https://doi.org/10.1080/10934529.2016.1229931>.

Rodea-Palomares, I., Leganés, F., Rosal, R., Fernández-Piñas, F., 2012. Toxicological interactions of perfluorooctane sulfonic acid (PFOS) and perfluorooctanoic acid (PFOA) with selected pollutants. *J. Hazard. Mater.* 201–202, 209–218. <https://doi.org/10.1016/j.jhazmat.2011.11.061>.

Santschi, P.H., Chin, W.-C., Quigg, A., Xu, C., Kamalanathan, M., Lin, P., et al., 2021. Marine gel interactions with hydrophilic and hydrophobic pollutants. *Gels* 7, 83. <https://doi.org/10.3390/gels7030083>.

Schloss, P.D., Westcott, S.L., Ryabin, T., Hall, J.R., Hartmann, M., Hollister, E.B., et al., 2009. Introducing mothur: open-source, platform-independent, community-supported software for describing and comparing microbial communities. *Appl. Environ. Microbiol.* 75, 7537–7541. <https://doi.org/10.1128/AEM.01541-09>.

Seymour, J.R., Amin, S.A., Raina, J.-B., Stocker, R., 2017. Zooming in on the phytoplankton-bacteria relationships. *Nat. Microbiol.* 2, 17065 <https://doi.org/10.1038/nmicrobiol.2017.65>.

Simpson, S.L., Liu, Y., Spadaro, D.A., Wang, X., Kookana, R.S., Batley, G.E., 2021. Chronic effects and thresholds for estuarine and marine benthic organism exposure to perfluoroctane sulfonic acid (PFOS)-contaminated sediments: influence of organic carbon and exposure routes. *Sci. Total Environ.* 776, 146008 <https://doi.org/10.1016/j.scitotenv.2021.146008>.

St, L., Wold, S., 1989. Analysis of variance (ANOVA). *Chemom. Intel. Lab. Syst.* 6, 259–272. [https://doi.org/10.1016/0169-7439\(89\)80095-4](https://doi.org/10.1016/0169-7439(89)80095-4).

Steichen, J.L., Labonté, J.M., Windham, R., Hala, D., Kaiser, K., Setta, S., et al., 2020. Microbial, physical, and chemical changes in Galveston Bay following an extreme flooding event, Hurricane Harvey. *Front. Mar. Sci.* 7, 186. <https://doi.org/10.3389/fmars.2020.00186>.

Stibet, A., 2013. Excitonic connectivity between photosystem II units: what is it, and how to measure it? *Photosynthetica Res.* 116, 189–214. <https://doi.org/10.1007/s11120-013-9863-9>.

Suggett, D., Moore, C., Hickman, A., Geider, R., 2009. Interpretation of fast repetition rate (FRR) fluorescence: signatures of phytoplankton community structure versus physiological state. *Mar. Ecol. Prog. Ser.* 376, 1–19. <https://doi.org/10.3354/meps07830>.

Sun, Y., Wang, T., Peng, X., Wang, P., Lu, Y., 2016. Bacterial community compositions in sediment polluted by perfluoroalkyl acids (PFAAs) using Illumina high-throughput sequencing. *Environ. Sci. Pollut. Res.* 23, 10556–10565. <https://doi.org/10.1007/s11356-016-6055-0>.

Sylvan, J.B., Quigg, A., Tozzi, S., Ammerman, J.W., 2007. Eutrophication-induced phosphorus limitation in the Mississippi River plume: evidence from fast repetition rate fluorometry. *Limnol. Oceanogr.* 52, 2679–2685. <https://doi.org/10.4319/lo.2007.52.6.2679>.

Tang, Z., Song, X., Xu, M., Yao, J., Ali, M., Wang, Q., et al., 2022. Effects of co-occurrence of PFASs and chlorinated aliphatic hydrocarbons on microbial communities in groundwater: a field study. *J. Hazard. Mater.* 435, 128969 <https://doi.org/10.1016/j.jhazmat.2022.128969>.

Taylor, J.D., Cunliffe, M., 2017. Coastal bacterioplankton community response to diatom-derived polysaccharide microgels: polysaccharide microgels and coastal bacterioplankton. *Environ. Microbiol. Rep.* 9, 151–157. <https://doi.org/10.1111/1758-2229.12513>.

Tukey, J.W., 1949. Comparing individual means in the analysis of variance. *Biometrics* 5, 99. <https://doi.org/10.2307/3001913>.

U.S. EPA, 2022. PFAS structures in DSSTox from CompTox chemicals dashboard v2.3.0. Retrieved from. https://comptox.epa.gov/dashboard/chemical-lists/PFA_STRUCTV5.

Viticoski, R.L., Wang, D., Feltman, M.A., Mulabagal, V., Rogers, S.R., Blersch, D.M., et al., 2022. Spatial distribution and mass transport of Perfluoroalkyl Substances (PFAS) in surface water: a statewide evaluation of PFAS occurrence and fate in Alabama. *Sci. Total Environ.* 836, 155524 <https://doi.org/10.1016/j.scitotenv.2022.155524>.

Wickham, H., 2016. *ggplot 2: Elegant Graphics for Data Analysis*. Springer-Verlag.

Williams, A.K., Bacosa, H.P., Quigg, A., 2017. The impact of dissolved inorganic nitrogen and phosphorus on responses of microbial plankton to the Texas City "Y" oil spill in Galveston Bay, Texas (USA). *Mar. Pollut. Bull.* 121, 32–44. <https://doi.org/10.1016/j.marpolbul.2017.05.033>.

Wu, J., Hua, Z., Gu, L., 2021. Planktonic microbial responses to perfluorinated compound (PFC) pollution: integrating PFC distributions with community coalescence and metabolism. *Sci. Total Environ.* 788, 147743 <https://doi.org/10.1016/j.scitotenv.2021.147743>.

Wu, J., Hua, Z., Gu, L., Li, X., Gao, C., Liu, Y., 2022a. Perfluorinated compounds (PFCS) in regional industrial rivers: interactions between pollution flux and eukaryotic community phylosymbiosis. *Environ. Res.* 203, 111876 <https://doi.org/10.1016/j.envres.2021.111876>.

Wu, J.-Y., Gu, L., Hua, Z.-L., Wang, D.-W., Xu, R.-Y., Ge, X.-Y., et al., 2022b. Removal of per-, poly-fluoroalkyl substances (PFASs) and multi-biosphere community dynamics in a bacteria-algae symbiotic aquatic ecosystem. *Environ. Pollut.* 314, 120266 <https://doi.org/10.1016/j.envpol.2022.120266>.

Xu, D., Li, C., Chen, H., Shao, B., 2013. Cellular response of freshwater green algae to perfluoroctanoic acid toxicity. *Ecotoxicol. Environ. Saf.* 88, 103–107. <https://doi.org/10.1016/j.ecoenv.2012.10.027>.

Xu, D., Chen, X., Shao, B., 2017. Oxidative damage and cytotoxicity of perfluoroctane sulfonate on *Chlorella vulgaris*. *Bull. Environ. Contam. Toxicol.* 98, 127–132. <https://doi.org/10.1007/s00128-016-1957-6>.

Xue, X., Gao, N., Xu, F., 2022. Toxicity of perfluoroctane sulfonate (PFOS) and perfluorobutane sulfonate (PFBS) to *Scenedesmus obliquus*: photosynthetic characteristics, oxidative damage and transcriptome analysis. *Environ. Pollut.* 315, 120397 <https://doi.org/10.1016/j.envpol.2022.120397>.

Yan, W., Qian, T., Zhang, L., Wang, L., Zhou, Y., 2021. Interaction of perfluoroctanoic acid with extracellular polymeric substances - role of protein. *J. Hazard. Mater.* 401, 123381 <https://doi.org/10.1016/j.jhazmat.2020.123381>.

Yeager, C.M., Gallegos-Graves, L.V., Dunbar, J., Hesse, C.N., Daligault, H., Kuske, C.R., 2017. Polysaccharide degradation capability of actinomycetales soil isolates from a semiarid grassland of the Colorado Plateau. *Appl. Environ. Microbiol.* 83, e03020-16 <https://doi.org/10.1128/AEM.03020-16>.

Zäncker, B., Cunliffe, M., Engel, A., 2018. Bacterial community composition in the sea surface microlayer off the Peruvian coast. *Front. Microbiol.* 9, 2699. <https://doi.org/10.3389/fmicb.2018.02699>.

Zhang, Y., Qv, Z., Wang, J., Yang, Y., Chen, X., Wang, J., et al., 2022. Natural biofilm as a potential integrative sample for evaluating the contamination and impacts of PFAS on aquatic ecosystems. *Water Res.* 215, 118233 <https://doi.org/10.1016/j.watres.2022.118233>.

Zhang, L., Zheng, X., Liu, X., Li, J., Li, Y., Wang, Z., et al., 2023a. Toxic effects of three perfluorinated or polyfluorinated compounds (PFCS) on two strains of freshwater algae: implications for ecological risk assessments. *J. Environ. Sci.* 131, 48–58. <https://doi.org/10.1016/j.jes.2022.10.042>.

Zhang, M., Wang, Q., Song, X., Ali, M., Tang, Z., Liu, X., et al., 2023b. Co-occurrence of PFASs, heavy metals and PAHs and their composite impacts on microbial consortium in soil: a field study. *Pedosphere* S1002016023000632. <https://doi.org/10.1016/j.pedsph.2023.06.001>.

Zhao, Z., Zheng, X., Han, Z., Yang, S., Zhang, H., Lin, T., et al., 2023a. Response mechanisms of *Chlorella sorokiniana* to microplastics and PFOA stress: photosynthesis, oxidative stress, extracellular polymeric substances and antioxidant system. *Chemosphere* 323, 138256. <https://doi.org/10.1016/j.chemosphere.2023.138256>.

Zhao, Z., Zheng, X., Han, Z., Yang, S., Zhang, H., Lin, T., et al., 2023b. Response mechanisms of *Chlorella sorokiniana* to microplastics and PFOA stress: photosynthesis, oxidative stress, extracellular polymeric substances and antioxidant system. *Chemosphere* 323, 138256. <https://doi.org/10.1016/j.chemosphere.2023.138256>.